

Quantum Neural Networks

Sanjay Gupta

*Department of Computer Science, Virginia Polytechnic Institute and State University,
7054 Haycock Road, Falls Church, Virginia 22043-2311
E-mail: sgupta@vt.edu*

and

R. K. P. Zia

*Department of Physics, Virginia Polytechnic Institute and State University,
Blacksburg, Virginia 24061-0435
E-mail: rkpzia@vt.edu*

Received November 21, 2001; revised February 23, 2001

This paper initiates the study of quantum computing within the constraints of using a polylogarithmic ($O(\log^k n)$, $k \geq 1$) number of qubits and a polylogarithmic number of computation steps. The current research in the literature has focussed on using a polynomial number of qubits. A new mathematical model of computation called *Quantum Neural Networks* (*QNNs*) is defined, building on Deutsch's model of quantum computational network. The model introduces a nonlinear and irreversible gate, similar to the speculative operator defined by Abrams and Lloyd. The precise dynamics of this operator are defined and while giving examples in which nonlinear Schrödinger's equations are applied, we speculate on its possible implementation. The many practical problems associated with the current model of quantum computing are alleviated in the new model. It is shown that QNNs of logarithmic size and constant depth have the same computational power as threshold circuits, which are used for modeling neural networks. QNNs of polylogarithmic size and polylogarithmic depth can solve the problems in NC, the class of problems with theoretically fast parallel solutions. Thus, the new model may indeed provide an approach for building scalable parallel computers. © 2001 Elsevier Science (USA)

Key Words: theoretical computer science; parallel computation; quantum computing; Church–Turing thesis; threshold circuits.

1. INTRODUCTION

The concept of quantum computing, based on the quantum mechanical nature of physical reality, is first stated by Benioff [5] and Feynman [15], and formalized by

Deutsch [13], Bernstein and Vazirani [8], and Yao [42]. For background material, the reader is referred to the papers mentioned above, survey papers [2, 9, 33, 38], books [18, 41], and courses available on the web [29, 40].

Considerable interest has been generated in quantum computing since Shor [37] showed that numbers can be factored in polynomial time on a quantum computer. From a practical viewpoint, Shor's result shows that a working quantum computer can violate the security of transactions that use the RSA protocol, a standard for secure transactions on the Internet. From a theoretical viewpoint, the result seemingly violates the polynomial version of the Church–Turing thesis; it is generally believed that factoring cannot be done in polynomial time on a deterministic or probabilistic Turing machine. What makes Shor's breakthrough result possible on a quantum Turing machine is that exponentially many computations can be performed in parallel in one step and certain quantum steps enable one to extract the desired information.

Even though simple quantum computers have been built, enormous practical issues remain for larger scale machines. The problems seem to be exacerbated with more qubits and more computation steps. In this paper, we initiate the study of quantum computing within the constraints of using a polylogarithmic ($O(\log^k n)$, $k \geq 1$) number of qubits and a polylogarithmic number of computation steps. The current research in the literature has focussed on using a polynomial number of qubits. (Recently, researchers have initiated the study of quantum computing using a polynomial number of qubits and a polylogarithmic number of steps [12, 17, 27, 28]). We define a new mathematical model of computation called *Quantum Neural Networks* (QNNs), building on Deutsch's model of quantum computational network [14]. The new model introduces a nonlinear, irreversible, and dissipative operator, called D gate, similar to the speculative operator introduced by Abrams and Lloyd [1]. We also define the precise dynamics of this operator and while giving examples in which nonlinear Schrödinger's equations are applied, we speculate on the possible implementation of the D gate.

Within a general framework of size, depth, and precision complexity, we study the computational power of QNNs. We show that QNNs of logarithmic size and constant depth have the same computational power as threshold circuits, which are used for modeling neural networks. QNNs of polylogarithmic size and polylogarithmic depth can solve the problems in NC, the class of problems that have theoretically fast parallel solutions. Thus, the new model subsumes the computation power of various theoretical models of parallel computation.

We believe that the true advantage of quantum computation lies in overcoming the communication bottleneck that has plagued the implementation of various theoretical models of parallel computation. For example, NC circuits elegantly capture the class of problems that can be theoretically solved fast in parallel using simple gates. While fast implementations of individual gates have been achieved with semiconductors and millions of gates have been put on a single chip, we do not have the implementation of full NC circuits because of the communication and synchronization costs involved in wiring a polynomial number of gates. We believe that this hurdle can be overcome using the nonlocal interactions present in

quantum systems—there is no need to explicitly wire the entangled units and the synchronization is instantaneous. This advantage is manifest in the standard unitary operator, where operations on one qubit can affect probability amplitudes on all the qubits, without requiring explicit physical connections and a global clock. Thus, the new model has the potential to overcome the practical problems associated with both quantum computing as well as classical parallel computing.

The paper addresses three categories of researchers: complexity theory, neural networks, and quantum computing. For complexity theorists, the paper shows that the $2^{\log^{O(1)} n}$ bounds on threshold circuits obtained in various results such as [3] is not necessarily infeasible. (Polynomial time and space is generally accepted as defining feasible bounds.) For neural network researchers, the paper mathematically proves that threshold circuits used for modeling neural networks have the same computation power as the equality threshold circuits, introduced in this paper. The new class has certain algebraic advantages and it may indeed be beneficial to redo the theory of neural networks under this model. Finally, for quantum computing researchers, the paper shows that with quantum computing we can build scalable parallel computers, beyond the current digital technology, under very tight constraints. Of course, this depends on the physical realization of the inherently nonlinear gate introduced in the paper and thus it is worthwhile exploring its implementation. Furthermore, we do not need to limit ourselves to the fundamental linear models of systems to obtain useful devices; we should explore systems at a different level of abstractions that may not be defined by linear equations.

This paper is organized as follows: Section 2 summarizes the current model of quantum computing, together with the associated problems, including some new issues not discussed in the literature. Section 3 first defines a framework for new quantum computing models, based on the problems discussed in Section 2. The D gate is introduced within this framework. (This is the only speculative part of the paper; that is, we do not know how to implement the D gate.) QNNs are defined to be Deutsch's quantum computational network [14] together with the D gate.

Section 4 quantifies the computational power of the new model. We prove that equality threshold circuits have essentially the same computational power as the standard class of threshold circuits used for modeling neural networks. Then QNNs are shown to have the same computational power as equality threshold gates. Section 5 defines the precise dynamics of the D gate. Section 6 identifies some of the many nonlinearities in quantum systems. Finally, Section 7 delineates many interesting research directions suggested by this paper.

2. CURRENT MODEL OF QUANTUM COMPUTING

There are two equivalent models for quantum computing, quantum Turing machines [8, 13] based on reversible Turing machines [6, 7] and quantum computational network [14]. Our model builds on the latter, so we briefly review it here. The basic unit in quantum computation is a *qubit*, a superposition of two independent states $|0\rangle$ and $|1\rangle$, denoted $\alpha_0 |0\rangle + \alpha_1 |1\rangle$, where α_0, α_1 are complex numbers such that $|\alpha_0|^2 + |\alpha_1|^2 = 1$. A system with n qubits is described using 2^n independent

states $|i\rangle$, $0 \leq i \leq 2^n - 1$, each associated with *probability amplitude* α_i , a complex number, as follows: $\sum_{i=0}^{2^n-1} \alpha_i |i\rangle$ where $\sum_{i=0}^{2^n-1} |\alpha_i|^2 = 1$. The direction of α_i on the complex plane is called the *phase* of state $|i\rangle$ and the absolute value $|\alpha_i|$ is called the *amplitude* of state $|i\rangle$.

The computation unit in Deutsch's model consists of *quantum gates* whose inputs and outputs are qubits. A gate can perform any local unitary operation on the inputs. It has been shown that one-qubit gates together with two-qubit controlled NOT gates are universal [4].

The quantum gates are interconnected by *wires*. A quantum computational network is a computing machine consisting of quantum gates with synchronized steps. By convention, the computation proceeds from left to right. The outputs of some of the gates are connected to the inputs of others. Some of the inputs are used as the input to the network. Other inputs are connected to *source* gates for 0 and 1 qubits. Some of the outputs are connected to *sink* gates, where the arriving qubits are discarded. The essential ingredients of the model are summarized in Fig. 1. An output qubit can be measured along state $|0\rangle$ or $|1\rangle$ and is observed based on the probability amplitudes associated with the qubit.

Even though simple quantum computers have been built, enormous practical issues remain for larger scale machines. Landauer [23] exposes three main problems: *decoherence*, *localization*, and *manufacturing defects*. Decoherence is the process by which a quantum system decays to a classical state through interaction with the environment. In the best case, coherence is maintained for some 10^4 s, and, in the worst case, for about 10^{-10} s for single qubits. Some decoherence models show the coherence time declining exponentially as the number of qubits increases [39]. Furthermore, the physical media that allow fast operations are also the ones with short coherence times.

The computation may also suffer from localization, that is, from reflection of the computational trajectory, causing the computation to turn around. Landauer [23] points out that this problem is largely ignored by the research community. The combination of decoherence and localization makes the physical realization of quantum computation particularly difficult. On the one hand, we need to isolate a quantum computing system from the environment to avoid decoherence, and on the other hand, we need to control it externally to compel it to run forward to avoid reflection. Finally, minor manufacturing defects can engender major errors in the computations.

Introduction of the techniques of error-correcting codes and fault-tolerant computation to quantum computation has generated considerable optimism for

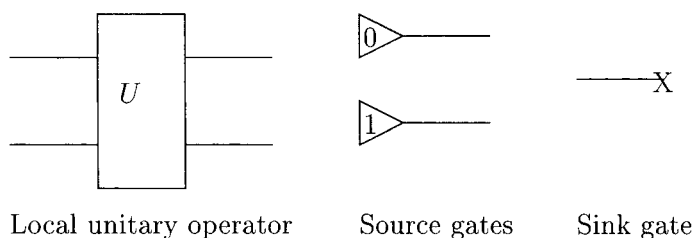


FIG. 1. Components of Deutsch's quantum computational network model.

building quantum computers, because these techniques can alleviate the problems of decoherence and manufacturing defects. Though this line of research is elegant and exciting, the codes correct only local errors. For example, one qubit can be encoded into the nonlocal interactions among three qubits to correct one qubit errors. However, in principle, any (nonlocal) unitary operator can be applied to all the qubits. These nonlocal errors easily subvert the error-correcting codes. Also, nonlocal interactions provide the exponential speed-ups in quantum computing. The hope that nature might allow computational speed-ups via nonlocal interactions, while errors are constrained to occur only locally, seems unavailing. For an excellent exposition on error-correcting codes and fault-tolerant quantum computing, the reader is referred to [30].

It has been shown that one-qubit gates together with two-qubit controlled NOT gates are universal [4]; that is, any $2^n \times 2^n$ unitary operator can be decomposed into a polynomial number of one and two qubit operators. However, in general, any error operator can be applied in one step that cannot even be detected without observing all the involved qubits. Having the ability to operate on many qubits does not solve the problem, for error-correcting codes for k qubit errors can be subverted by a $(k+1)$ -qubit error operator. Eventually, construction of a $2^n \times 2^n$ operator will itself be more time consuming than the actual computation.

There are some additional difficulties with computing using a polynomial number of qubits for a polynomial number of steps that are not discussed in the literature. For example, if $n = 1000$ and an $O(n^2)$ quantum algorithm is used, we need one million *uniquely identifiable* but *identical* carriers of quantum information. Clearly, the carriers need to be uniquely identifiable because we are not using their statistical properties, but encoding $2^{O(n^2)}$ computations in their interactions. However, the carriers need to be absolutely identical for the following reason. In describing the Hamiltonian for the whole system, there is a phase oscillation associated with each carrier. If all carriers have the same frequency, it does not affect the computation, which essentially changes the state relative to the global oscillation. But each qubit is likely to be encoded in carriers with a much larger state space, and even slight frequency differences can result in substantial errors over a polynomial number of steps. The task of preparing one million absolutely identical carriers, while exploiting the 2^{10^6} interactions, most of which are nonlocal, for speeding-up computation appears insurmountable.

In conclusion, controlling a polynomial number of entangled qubits for a polynomial number of steps, while compelling the computation forward, seems hard even with the help of error-correcting codes. To address the above problems, we initiate the study of quantum computation under the constraints of a polylogarithmic number of qubits and a polylogarithmic number of steps.

3. QUANTUM NEURAL NETWORKS (QNNs)

In the previous section we saw that the problems with the current model get worse as the number of qubits and computation steps increase. Therefore, we make the following premises for a new model.

- The computation should be achieved within a few ($O(\log^k n)$, $k \geq 1$) steps.
- (Optional) The computation should use only a few ($O(\log^k n)$, $k \geq 1$) qubits.
- There should be irreversible synchronization points in the computation to avoid the problem of localization.

The second point is optional because a single particle, in principle, can encode an infinite amount of discrete information, for example, in spins $-s/2$, $-(s-1)/2$, ..., $s/2$ for any number s . Thus, many qubits can be encoded within a single particle, and hence, it may be worthwhile exploring models that use many qubits encoded on a few carriers. However, in this paper we observe all the above premises. Note that within the framework of our premises, quantum computation does not seem to violate the polynomial version of the Church–Turing thesis.

The next question is what operations should we have besides the standard unitary operator. In particular, what irreversible, and hence, nonlinear operators can be exploited for computation. In its present formulation, quantum mechanics for an isolated system, or one interacting with *classical* external potentials, is linear in the state vector. However, if full interactions with an environment are taken into account, then their effects can be found by projecting the larger state vector of the combined system into the subspace of our system alone. As a result, the evolution equation for the latter state vector is not necessarily linear. The behavior of a system can also be nonlinear because of the interactions between the degrees of freedom, as discussed in Section 6.

In general, these nonlinear operations can be on the phases as well as amplitudes (or both) associated with a quantum system. The phases in a quantum system have the following properties.

- Phases cannot be directly observed.
- They have an oscillation associated with them.
- Quantum mechanics can be defined using a density matrix formulation, which is typically used when incorporating phase information is not feasible.

Therefore, it seems natural to have nonlinearities on amplitudes only. Specifically, we introduce a new nonlinear operator D gate (for dissipative) in Deutsch's quantum computational network model [14]. The operator $D(m, \delta)$, abbreviated D with threshold δ (Fig. 2), when applied to the m qubits in a system with $n \geq m$ qubits behaves as follows. Let the states of m qubits be represented by binary numbers 0 through $2^m - 1$ or, equivalently, binary strings 0^m through 1^m . Let $\mathcal{A}(|j\rangle)$ and $\mathcal{A}'(|j\rangle)$ respectively denote the probability amplitudes before and after the application of the D operator. Then,

$$|\mathcal{A}(|0^m\rangle)| < \delta \Rightarrow \mathcal{A}'(|0^m\rangle) = 0,$$

and

$$|\mathcal{A}(|0^m\rangle)| > \delta \Rightarrow \mathcal{A}'(|0^m\rangle) = c.$$

The value c for probability amplitude denotes some constant used for encoding 1. For example, if a system consists of n qubits, then $\mathcal{A}'(|0^m\rangle) = 1/\sqrt{2^n}$ is sufficient for the case $|\mathcal{A}(|0^m\rangle)| > \delta$. In this case, threshold δ is chosen so that $0 < \delta < 1/\sqrt{2^n}$. (From now on, we'll simply use 1 instead of c .) Note that the behavior of the D gate is undefined on all the states except $|0^m\rangle$. In this paper, it is irrelevant what happens to these states as the corresponding qubits go to a sink gate after the application of the D operator. Also, the behavior of the D gate at $|\mathcal{A}(|0^m\rangle)| = \delta$ is irrelevant in this paper.

If the m qubits passed through the D gate are part of a larger quantum system with $n > m$ qubits, then the D operator behaves as above for all amplitudes $\mathcal{A}(|j; 0^m\rangle)$, where j , $0 \leq j \leq 2^{n-m}$. Thus, amplitudes of different states $|j; 0^m\rangle$ converge to 0 or 1 depending on the initial value of $\mathcal{A}(|j; 0^m\rangle)$, independently of each other.

In practice, only an approximate behavior of D may be realizable within finite convergence time (Fig. 2). This can be sufficient, depending on the circuit which uses the gate. We will see that δ_0 , δ , and δ_1 are defined by the types of problems we are trying to solve.

The D gate can be intuitively thought of as a contractive operator that evolves general states towards a single (stable) state $|0^m\rangle$. Clearly, it cannot be realized in an isolated system where the only permissible operators are unitary. However, as discussed before, a truly isolated system is, in any case, a theoretical ideal which is difficult to realize in practice. In Section 5, we see that the D gate needs inherently nonlinear behavior as well as dissipative behavior. It is similar to the speculative operator defined by Abrams and Lloyd [1]; however, the nonlinearity depends only on the amplitude and not on phases.

To meet the requirement of having at most a polylogarithmic number of qubits, we use a dense encoding of n classical bits, labelled x_0, \dots, x_{n-1} , in only $O(\log n)$ qubits. There are several alternatives. The following simple one suffices. Assume n is a power of 2. Interpret the states of $\log n$ qubits as addresses and if the j th classical bit is 1, then $\mathcal{A}(|j\rangle) = 1$, else $\mathcal{A}(|j\rangle) = 0$. As before, the value 1 represents some appropriate constant c ; if the system has $\log n$ qubits, $c = 1/\sqrt{n}$ is sufficient.

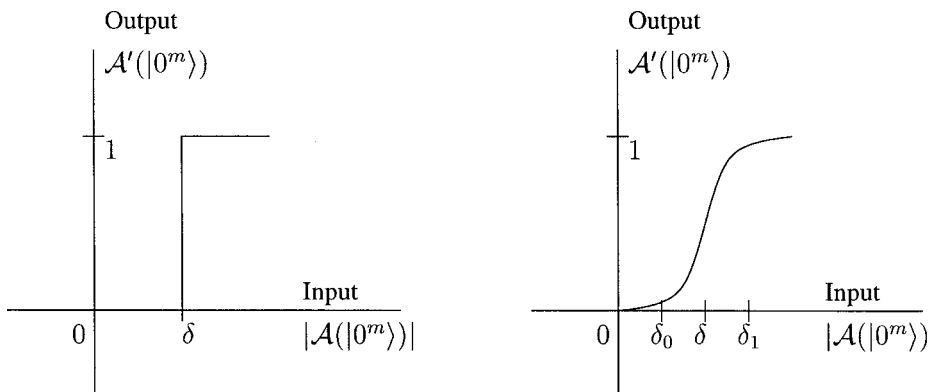


FIG. 2. Behavior of $D(m, \delta)$ gate: (left) ideal gate, (right) approximate gate.

We include a special *sink state* z so that the probabilities add to 1. Thus, $|\mathcal{A}(|z\rangle)|^2 = 1 - \sum_{j=0}^{n-1} |\mathcal{A}(|j\rangle)|^2$. The sink state may be composed of several states. For example, if we think of the sink state as an additional qubit, then $\mathcal{A}(|j; 0\rangle)$ can be used for encoding 0 and 1, and $\sum_{j=0}^{n-1} |\mathcal{A}(|j; 1\rangle)|^2 = 1 - \sum_{j=0}^{n-1} |\mathcal{A}(|j; 0\rangle)|^2$.

As in Deutsch's quantum computational network model [14], our model has *quantum gates* interconnected by *wires*. In particular, we preserve *source* and *sink* gates.¹ Our model also has the standard reversible unitary operator U . Since we are working within the constraints of polylogarithmic qubits, we allow arbitrary unitary operators.² Of course, a unitary operator of dimension $2^{\log^k n}$, $k \geq 1$, can be approximated by decomposition into $\log^k n$, $k \geq 1$, local operators using standard techniques [4]. However, in principle, any unitary matrix is allowed in quantum mechanics. We say that a U gate has *precision* p if all the values in the matrix can be approximated to within $1/2^{p+1}$ by binary rational numbers.

The unitary operator implicitly contains the important properties that overcome the main problems with classical parallel computing: communication bottleneck and synchronization overhead. Because of entanglement, operations on even one qubit can affect all the qubits instantaneously, without the need for explicitly wiring them together. While the research in literature has focussed on exploiting the exponential properties of quantum systems to perform computations infeasible with the current digital systems, our model is using only the entanglement and interference present in quantum systems to overcome the communication bottleneck and synchronization problems that have plagued the implementation of parallel computers. We believe that scalable parallel computers can be built using quantum systems.

A *quantum neural network* $QNN(s(n), d(n))$ of precision $p(n)$ is a circuit of size $s(n)$ and depth $d(n)$, constructed from the gates D and U of precision $p(n)$. Size denotes the number of qubits in the circuit and depth denotes the longest sequence of gates from input to output. In general, the reversible U gate is followed by the irreversible D gate to eliminate the problem of localization. Usually, the precision of the circuits will be $O(s(n))$.

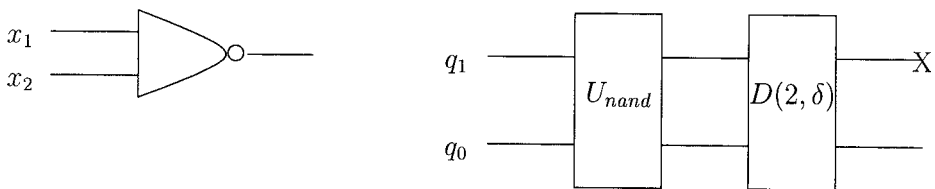
Size, depth, and precision are important complexity-theoretic measures that quantify various aspects of computations. Depth corresponds to the number of steps needed to solve a given problem. Size usually corresponds to the size of apparatus; precision also characterizes the apparatus needed for solving the problem.

3.1. Examples of QNNs

We give examples of QNNs for some simple circuits with the universal NAND gates. Define a unitary matrix U_{nand} that operates on two qubits as follows.

¹ When a qubit goes to a sink gate, it is measured to remove the entanglements with the remaining qubits.

² With polynomial number of qubits, if we allow arbitrary unitary operators (of size $2^n \times 2^n$), then the cost of constructing the apparatus can defeat the gains in computational speed.


 FIG. 3. QNN for $\text{NAND}(x_1, x_2)$.

$$U_{nand} = \begin{bmatrix} \frac{1}{\sqrt{6}} & 0 & \frac{1}{\sqrt{6}} & \frac{-2}{\sqrt{6}} \\ \frac{1}{\sqrt{3}} & \frac{1}{\sqrt{3}} & -\frac{1}{\sqrt{3}} & 0 \\ \frac{1}{3\sqrt{2}} & \frac{\sqrt{2}}{3} & \frac{1}{\sqrt{2}} & \frac{\sqrt{2}}{3} \\ \frac{2}{3} & -\frac{2}{3} & 0 & \frac{2}{6} \end{bmatrix} \begin{matrix} |00\rangle \\ |01\rangle \\ |10\rangle \\ |11\rangle \end{matrix} \quad X = \frac{1}{2} \begin{bmatrix} x_1 \\ 1 \\ x_2 \\ 1 \end{bmatrix}$$

In the input vector X , 0 is encoded as 0 and 1 is encoded as $1/2$. The amplitude of the state $|00\rangle$ in the state vector $U_{nand}X$ is 0 if and only if $\text{NAND}(x_1, x_2) = 0$. Thus, when we pass the qubits through a $D(2, \delta)$ gate with $0 < \delta < 1/2\sqrt{6}$, the amplitude of state $|00\rangle$ has the correct answer (Fig. 3). We have not included the sink state in the above description.

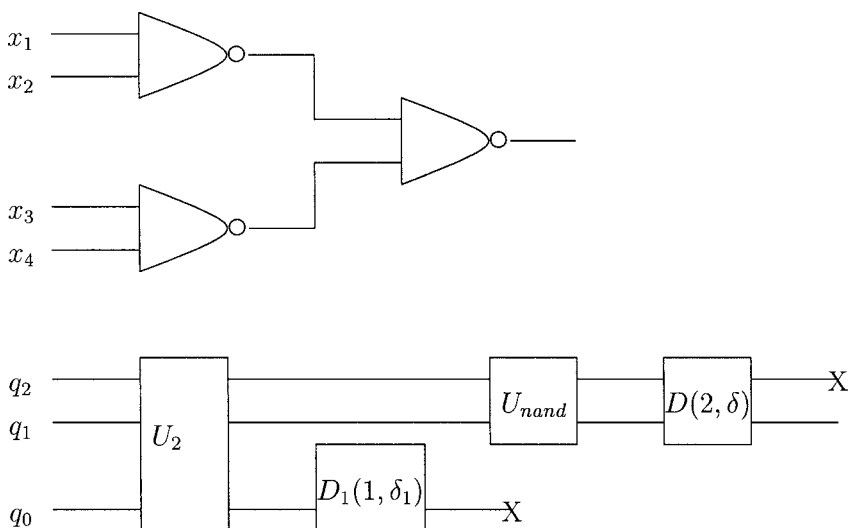


FIG. 4. QNN for a circuit with NAND gates.

Next we show how a circuit with three NAND gates can be simulated by a QNN (see Fig. 4). Define U_2 to be the following unitary matrix.

$$U_2 = \begin{bmatrix} U_{nand} & \mathbf{0} \\ \mathbf{0} & U_{nand} \end{bmatrix}_{8 \times 8}$$

The operator U_2 operates on $X^T = 1/\sqrt{8} [x_1, 1, x_2, 1, x_3, 1, x_4, 1]$. When the result is passed through the $D_1(1, \delta_1)$ gate, $0 < \delta_1 < 1/\sqrt{6 \cdot 8}$, we simulate the two NAND gates simultaneously. The resulting vector is $[\text{NAND}(x_1, x_2), 1, \text{NAND}(x_3, x_4), 1]$, which is used to simulate the last NAND gate as before. As an aside, the construction of QNNs for arbitrary circuits of NAND gates, given in Section 4, is different from the construction given in Fig. 4 and has worse bounds.

4. COMPUTATIONAL POWER OF QNNs

In this section, we characterize the computational power of QNNs using the known results from the complexity theory of parallel computations and threshold circuits (used for modeling neural networks [25, 26]). First, we define a class of circuits called EC and show that with polynomial size they have the same computational power as threshold circuits. EC circuits can be converted into QNNs using a proper encoding of classical bits into qubits.

4.1. Circuits

Let G be a set of gates (functions) that map several bits to one bit. For each $n \geq 0$, a circuit C_n over the set G is a directed, acyclic graph with a list of input nodes (with no incoming edges), a list of output nodes (with no outgoing edges), and a gate in G labeling each noninput node. Given a binary input string (x_1, \dots, x_n) , we label each input node x_i or \bar{x}_i (NOT x_i). For every other node v with m predecessors y_1, \dots, y_m , we recursively assign a value $g(y_1, \dots, y_m)$, where g is the gate that labels node v . C_n outputs the value given by the list of output nodes.

Unless otherwise stated, in this paper, we shall allow the circuits to have arbitrary fan-in and fan-out. Circuits with fan-out 1 will be called “opened circuits,” where the corresponding graph is a tree. The *size* of a circuit C_n is the number of nodes in C_n , and the *depth* of C_n is the length of the longest path from any input node to an output node.

A *circuit family* is an infinite list of circuits $\mathbf{C} = (C_1, C_2, \dots, C_n, \dots)$, where C_n has n binary inputs. \mathbf{C} computes a family of boolean functions $(f_1, f_2, \dots, f_n, \dots)$, where f_n is the boolean function computed by circuit C_n . We say that \mathbf{C} has *size complexity* $s(n)$ and *depth complexity* $d(n)$ if for all $n \geq 0$ circuit C_n has size at most $s(n)$ and depth at most $d(n)$. Size and depth are important complexity descriptions of circuits that respectively characterize the size of apparatus and the number of steps needed to compute a family of boolean functions.

A circuit family is *polytime-uniform* if there exists a Turing machine with time bound n^k , $k \geq 1$, that constructs circuit C_n on input 1^n . A circuit family is *logspace-uniform* if there exists a Turing machine with space bound $\log n$ that constructs circuit C_n , on input 1^n . Uniformity conditions capture the complexity of constructing the circuit to compute boolean functions with inputs of a given size.

4.2. Threshold Circuits

A *threshold function* with threshold Δ is a boolean function denoted $Th^{n,\Delta}$: $\{0, 1\}^n \rightarrow \{0, 1\}$ such that

$$Th^{n,\Delta}(x_1, \dots, x_n) = \begin{cases} 1 & \text{if } \sum_{i=1}^n x_i \geq \Delta \\ 0 & \text{otherwise} \end{cases}$$

for $x_1, \dots, x_n \in \{0, 1\}$, where $0 \leq \Delta \leq n$. A *weighted threshold function* of weight bound w and threshold Δ is a boolean function denoted $Th_{w_1, \dots, w_n}^{n,\Delta} : \{0, 1\}^n \rightarrow \{0, 1\}$ such that

$$Th_{w_1, \dots, w_n}^{n,\Delta}(x_1, \dots, x_n) = \begin{cases} 1 & \text{if } \sum_{i=1}^n w_i x_i \geq \Delta \\ 0 & \text{otherwise,} \end{cases}$$

for $w_1, \dots, w_n, \Delta \in \mathcal{Z}$ (set of integers), $|w_i| \leq w$ for all i , and $x_1, \dots, x_n \in \{0, 1\}$.

A *threshold circuit* is a circuit over the set of threshold gates. Let $TC(s(n), d(n))$ denote the collection of threshold circuits of size $s(n)$ and depth $d(n)$. We overload the notation TC to also denote the class of functions computable by these circuits. *Weighted* $TC(s(n), d(n))$ of weight bound w denotes the collection of threshold circuits using weighted threshold gates of weight bound w of size $s(n)$ and depth $d(n)$.

THEOREM 4.1. [32] *Suppose an analytic function $f(x)$ has a convergent Taylor series expansion $f(x) = \sum_{n=0}^{\infty} c_n(x-x_0)^n$ over an interval $|x-x_0| \leq \varepsilon$ where $0 < \varepsilon < 1$, and the coefficients are rationals $c_n = a_n/b_n$ where a_n, b_n , are integers of magnitude at most $2^{n^{O(1)}}$. Then polytime-uniform threshold circuits of polynomial size and simultaneous constant depth can compute $f(x)$ over this interval within accuracy 2^{-n^c} for any constant $c \geq 1$.*

The above theorem implies that $TC(n^{O(1)}, O(1))$ can approximate elementary functions such as sine, cosine, exponential, logarithm, and square root. $TC(n^{O(1)}, O(1))$ can also exactly compute integer and polynomial quotient and remainder, interpolation of rational polynomials, banded matrix inverse, and triangular Toeplitz matrix inverse [32].

4.3. Equality (Threshold) Circuits

A (weighted) equality threshold function of weight bound $w \geq 0$ is a boolean function denoted $Et_{w_1, \dots, w_n}^n : \{0, 1\}^n \rightarrow \{0, 1\}$ such that

$$Et_{w_1, \dots, w_n}^n(x_1, \dots, x_n) = \begin{cases} 0 & \text{if } \sum_{i=1}^n w_i x_i = 0 \\ 1 & \text{otherwise,} \end{cases}$$

for $w_1, \dots, w_n \in \mathcal{L}$, $|w_i| \leq w$ for all i , and $x_1, \dots, x_n \in \{0, 1\}$. Note that Et gates possess an elegant algebraic structure as they can be naturally generalized to any domain, such as complex numbers.

An *equality threshold circuit* of weight bound w is a circuit over the set of equality threshold gates such that all the weights are absolutely bounded by w . Let $EC(s(n), d(n))$ denote the collection of equality circuits of size $s(n)$ and depth $d(n)$. EC will also be used to denote the class of functions computable by these circuits.

We will see that the weights of a EC circuit can be encoded appropriately in unitary matrices, and quantum entanglement and interference can be used to compute $\sum_{j=1}^n w_j x_j$ in one step. Thus, EC provides a good model to help combine ideas from quantum computing and threshold circuits.

4.4. AND-OR Circuits

NC is the collection of logspace-uniform circuits of size $n^{O(1)}$ and depth $(\log n)^{O(1)}$ over the set $\{\text{AND}, \text{OR}\}$ of gates with fan-in bounded by 2. It is the class of problems that can theoretically be solved efficiently in parallel and contains numerous natural problems. We write NC to denote both the class of circuits and functions computable by the circuits. NC^i , $i \geq 1$, denotes the subclass of NC where the depth is limited to $O(\log^i n)$. Though NC circuits use remarkably fast AND, OR gates, the implementations of circuits have not been successful because of the communication bottleneck and synchronization cost involved in wiring a polynomial number of processors. The algorithms that show that problems are in NC are typically not used to solve problems in parallel; new algorithms are designed depending on the parallel architecture model that takes communication cost into account.

NC^1 is known to have several natural problems such as integer arithmetic and matrix multiplication. NC^2 includes matrix inverses and matrix rank computation as well. Please see any standard text such as [22] and [31] for more details.

4.5. Computational Power of TC and EC Circuits

We now show that TC and EC circuits have essentially the same computational power if we consider circuits of polynomial size. In all our constructions, if the original circuits are polytime-uniform and logspace-uniform, the constructed circuits are also polytime-uniform and logspace-uniform, respectively.

LEMMA 4.2. 1. $Th^{n,4}(x_1, \dots, x_n)$ can be simulated by $EC(O(n), 2)$ of weight bound $O(n)$.

2. $TC(s(n), d(n)) \subseteq EC(O(s^3(n)), d(n)+1)$ of weight bound $O(s^2(n))$, and $TC(s(n), d(n)) \subseteq EC(O(s^2(n)), 2d(n))$ of weight bound $O(s(n))$.

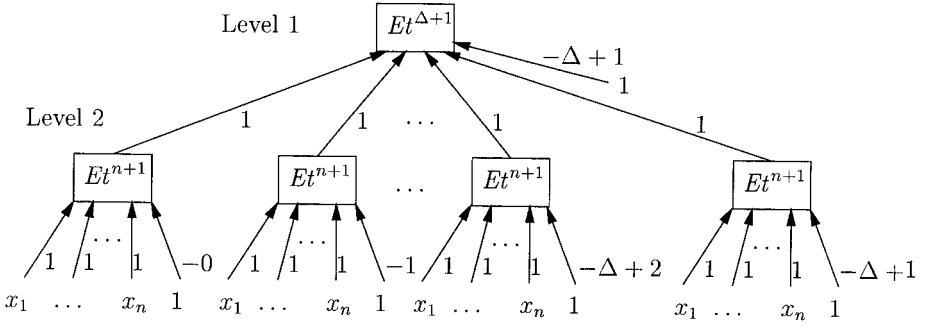


FIG. 5. Simulation of Threshold gate $Th^{n,\Delta}$ by EC of weight bound $O(n)$.

Proof. 1. Figure 5 shows the EC circuit that simulates the threshold gate $Th^{n,\Delta}(x_1, x_2, \dots, x_n)$. Note that the gates at level 2 check whether $\sum_{i=1}^n x_i$ is one of the values $0, 1, \dots, \Delta-1$, respectively.

Case ($\sum_{i=1}^n x_i < \Delta$). Exactly one gate at level 2 outputs 0 and all others output 1 giving the cumulative output of $\Delta-1$, which when combined with the input $-\Delta+1$ at level 1 gives the output of 0.

Case ($\sum_{i=1}^n x_i \geq \Delta$). All the gates at level 2 output 1 giving the cumulative output of Δ , which when added to the $-\Delta+1$ input at level 1 gives the final output of 1.

Thus, the cumulative output of gates at level 2 is Δ and $\Delta-1$ if the threshold gate outputs 1 and 0, respectively. The level 1 gate is used to add the outputs of gates at level 2 and subtract $\Delta-1$ from this sum.

The weight bound of the constructed circuit is $|-\Delta+1| = O(n)$.

2. An obvious replacement of each threshold gate by the circuit of Fig. 5 gives a depth of $2d(n)$ and size $O(s^2(n))$. We can reduce this bound to $d(n)+1$. Consider a threshold gate Th^{m_2, Δ_2} connected to another threshold gate Th^{m_1, Δ_1} . Figure 6 shows how the threshold gate at level 2 can be replaced by the equality threshold gates at level 2 described in Fig 5. Since the cumulative output of these equality threshold gates is Δ_2 and Δ_2-1 instead of 1 and 0, we simply increase the threshold of the level 1 gate of Fig. 6 by Δ_2-1 . It is easy to see that this replacement does not affect the function computed by the circuit.

The construction is as follows. Starting at the input level of TC circuit, replace each threshold gate as described above and adjust the threshold at the next level appropriately. Repeat the process for all levels. At the output level, use both level 1 and 2 gates of Fig. 5 so that the final gate is also a Et gate. As shown in Fig. 6, connect the new gates to all the gates connected by the replaced threshold gate.

Since the maximum threshold for all the threshold gates is bounded by $s^2(n)$ and each threshold gate is replaced by Δ Et gates, the final circuit has $O(s^3(n))$ Et gates.

The weight bound for the circuit is $O(s^2(n))$ because at the output level, the thresholds of all the $s(n)$ threshold gates are added together. ■

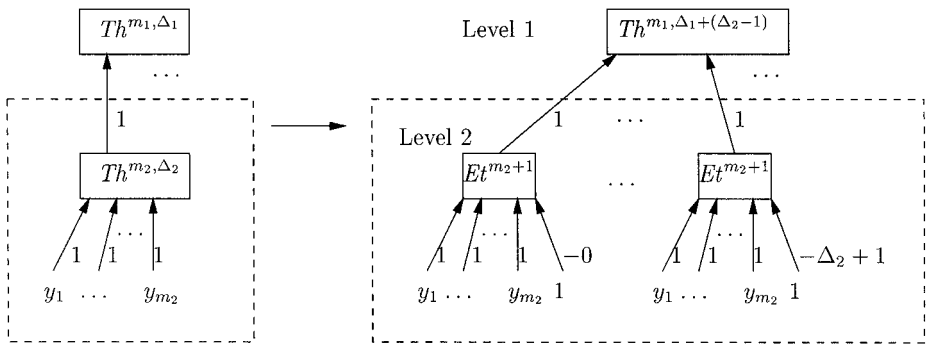


FIG. 6. Simulation of TC with EC.

LEMMA 4.3. 1. $Et^n_{w_1, \dots, w_n}(x_1, \dots, x_n)$ can be simulated by weighted TC(3, 2) of weight bound $\max(|w_1|, \dots, |w_n|)$.

2. $EC(s(n), d(n))$ of weight bound $w \subseteq \text{Weighted TC}(2s(n) + o, d(n) + 1)$ of weight bound w , where o is the number of output nodes in the $EC(s(n), d(n))$ circuit.

Proof. 1. Figure 7 shows the TC(3, 2) circuit that simulates the gate $Et^n_{w_1, \dots, w_n}(x_1, \dots, x_n)$. The leftmost gate at level 2 outputs 1 if $\sum_{i=1}^n w_i x_i \geq 1$ and the rightmost gate outputs 1 if $\sum_{i=1}^n w_i x_i \leq -1$. The gate at level 1 adds the two outputs from level 1 gates and outputs 0 if and only if $\sum_{i=1}^n w_i x_i = 0$.

2. An obvious replacement using Fig. 7 gives a circuit of depth $2d(n)$. We can reduce this bound to $d(n) + 1$. Consider an equality threshold gate Et^{m_2} connected to another equality threshold gate Et^{m_1} . Figure 8 shows how the equality threshold gate at level 2 can be replaced by the equality threshold gates at level 2 described in Fig. 7.

The construction is as follows. Starting at the input level of EC circuit, replace each Et gate with the level 2 threshold gates given in Fig. 7. Repeat the process until the output level. At the output level, use both level 1 and 2 gates of Fig. 7 so that the final gate is also a Th gate. As shown in Fig. 8, connect the new gates to all the gates connected by the replaced threshold gate.

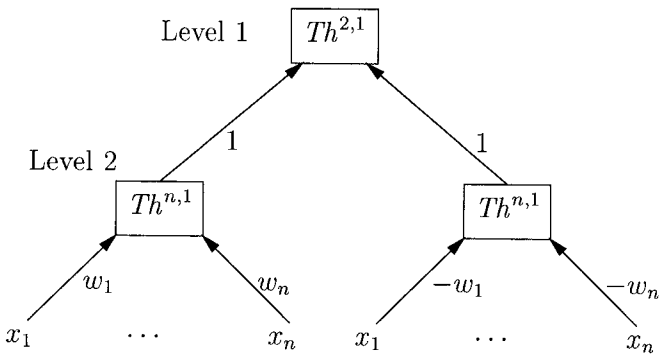


FIG. 7. Simulation of Equality threshold gate Et^n by weighted TC(3, 2).

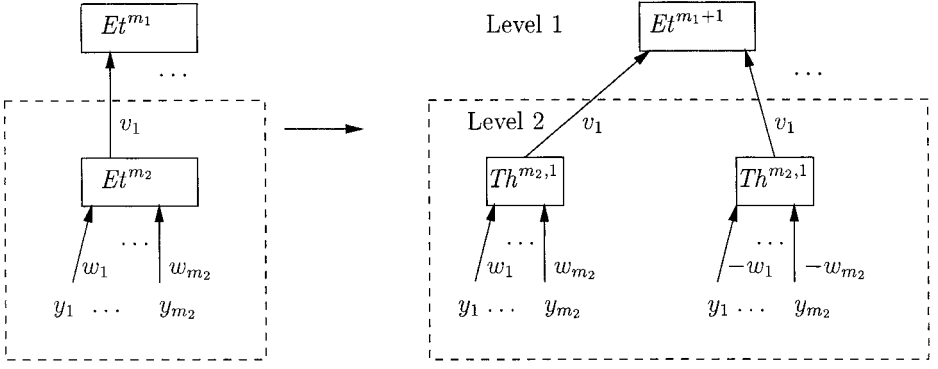


FIG. 8. Simulation of EC with TC.

Each Et gate is replaced by two Th gates except at the output level where each Et gate is replaced by 3 Th gates.

Since we do not change the absolute value of the weights, therefore the weight bound of the new circuit is the same as that of the original circuit. ■

LEMMA 4.4. *Weighted TC($s(n)$, $d(n)$) of weight bound $w \subseteq TC(O(w \cdot s(n))$, $d(n)$).*

Proof. 1. Suppose a threshold gate A is connected to another gate B with an edge with weight $w_{AB} \geq 0$. Simply make w_{AB} copies of gate A and connect them to gate B using an edge of weight 1. In general, we need at most $w \cdot s(n)$ copies.

Edges of weight 0 can be removed from the circuit. If a particular edge weight is negative, we can make it positive using the following standard technique.

Repeat the following steps for all gates at all levels starting from the output level down to the input level.

(a) If any weight $w_i < 0$ is negative, replace the weight with $-w_i > 0$ and the corresponding input x_i with $1 - x_i$ as shown in Fig. 9. Decrease the threshold of the gate by w_1 . Thus, $\sum_{i=1}^m w_i x_i \geq \Delta$ if and only if $-w_1(1 - x_1) + \sum_{i=2}^m w_i x_i \geq \Delta - w_1$.

With this step, some gates at intermediate levels may have two labels x_i and $1 - x_i$. If this is the case, duplicate the gate labelling one x_i and the other $1 - x_i$ retaining all the input connections. In the worst case, we double the number of gates.

(b) To complement the output of a gate from y to $1 - y$, use the process shown in Fig. 10. Replace all the weights w_i with $-w_i$ and change the threshold to

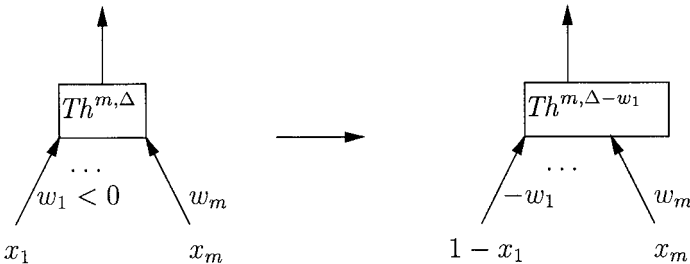


FIG. 9. Making weights positive by complementing input.

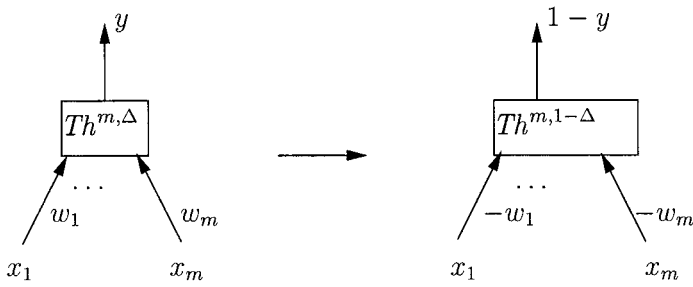


FIG. 10. Complementing output by negating weights.

$1 - \Delta$. Thus, the gate outputs $1 - y$ if and only if $\sum_{i=1}^m w_i x_i < \Delta$ if and only if $-\sum_{i=1}^m w_i x_i > -\Delta$ if and only if $\sum_{i=1}^m (-w_i) x_i \geq 1 - \Delta$.

When the input level is reached, change x_i to \bar{x}_i and vice versa as needed. The above process does not change the weight bound of the circuit. ■

LEMMA 4.5. 1. $\text{NAND}(x_1, x_2)$ can be simulated by $Et_{1,1,-2}^3(x_1, x_2, 1)$.

2. For all $i \geq 1$, $\text{NC}^i \subseteq \text{EC}(n^{O(1)}, O(\log^i n))$ of weight bound 2.

3. [34] $\text{SPACE}(s(n)) \subseteq \text{AND-OR}$ circuits of size $2^{s(n)}$ and depth $s^2(n)$ via $s^2(n)$ -uniform space-bounded Turing machines.

Proof. 1. Follows immediately from the definitions.

2. Since NAND gate is a universal gate, it can be used in place of AND and OR gates for NC circuits. Then, use the $Et_{1,1,-2}^3(x_1, x_2, 1)$ gate to simulate NAND gates. ■

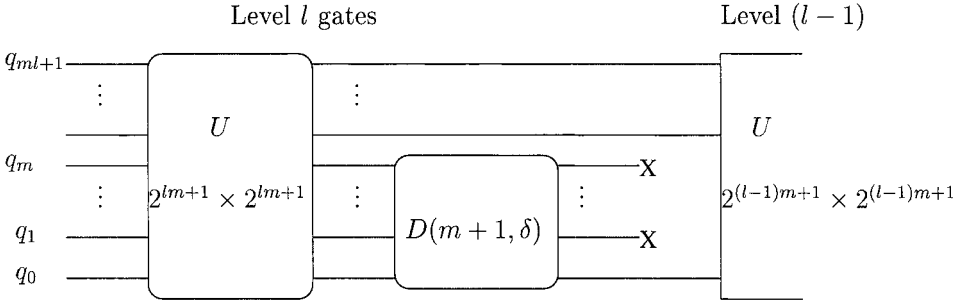
We are now ready to characterize the computational power of QNNs. Recall that the precision denotes the number of bits used for characterizing the amplitudes. Thus, if an amplitude is defined with precision p , then the actual value may differ by $1/2^{p+1}$, that is, the errors must be less than $1/2^{p+1}$.

THEOREM 4.6. $\text{EC}(s(n), d(n))$ of weight bound $w \subseteq \text{QNN}(O(d(n) \log s(n)), 2d(n))$ of precision $O(\log w + d(n) \log s(n))$.

Proof. For the sake of clarity, we write s and d instead of $s(n)$ and $d(n)$, respectively. Assume that all the gates have $s = 2^m$ inputs each; add inputs with weight 0, if necessary. Without loss of generality, we may assume that the circuits have one output. (Otherwise, connect all the output gates to another threshold gate and remove the corresponding layer in the constructed QNN.)

Given an unbounded fan-in, unbounded fan-out $\text{EC}(s, d)$ circuit of weight w , starting from the output gate “open” the circuit by duplicating gates of fan-out greater than 1 to obtain a new circuit. Add dummy gates to obtain a levelled circuit $\text{EC}(O(2^{md}), d)$.

Given this structured circuit, we will replace all the EC gates at level l by a U operator of size $2^{lm+1} \times 2^{lm+1}$ followed by a $D(m+1, \delta)$ operator (Fig. 11), where the threshold δ is specified below. Thus, we need a system with $md+1 = O(d \log s)$ qubits $q_0, q_1, \dots, q_{md}, q_{md+1}$. After each $D(m+1, \delta)$ operator, m qubits (except q_0) go

FIG. 11. QNN for level l of EC circuit.

to a sink gate so that we have only one qubit left after d levels of alternating U and D gates. Then this qubit is observed along state $|0\rangle$ to obtain the final answer.

For each level l of the EC circuit do the following.

1. Normalize the weights w_{jk} , $1 \leq k \leq s$, at each gate j by dividing them by $\sqrt{\sum_{k=1}^s |w_{jk}|^2}$. Since weights are bounded by w , therefore $\sqrt{\sum_{k=1}^s |w_{jk}|^2} \leq \sqrt{s} w$ and we require at least $O(\log s + \log w)$ precision for the weights. (To avoid the accumulation of errors as the computation proceeds through different levels, we will need slightly higher precision.)

2. Construct a banded matrix U of size $2^{lm+1} \times 2^{lm+1}$ and band width 2^{m+1} . For each gate j , $1 \leq j \leq 2^{m(l-1)}$, with normalized weights $w_{j1}, w_{j2}, \dots, w_{js}$, we have a block B_j in U .

The first row of B_j corresponds to the weights of gate j and the remaining rows are chosen so that the rows of B_j form a set of orthonormal vectors. The U matrix is the banded matrix with diagonal blocks $B_1, \dots, B_{2^{(l-1)m}}$. Note that the first row of block B_j computes the weighted sum $\sum_{k=1}^s w_{jk} x_{jk}$ for the j th gate if the input is $X^T = [x_{j1}, 0, x_{j2}, 0, \dots, x_{j2^m}, 0]$, $1 \leq j \leq 2^{m(l-1)}$. If we pass the $m+1 = \log s + 1$ least significant qubits through a $D(m+1, \delta)$ gate, we simulate all the Et gates at one level in parallel.

$$B_j = \begin{bmatrix} w_{j1} & 0 & w_{j2} & 0 & \cdots & w_{j2^m} & 0 \\ w_{j2^1} & w_{j2^2} & w_{j2^3} & w_{j2^4} & \cdots & w_{j2^{2^{m+1}-1}} & w_{j2^{2^{m+1}}} \\ & & & \cdots & & & \\ w_{j2^{m+1}1} & w_{j2^{m+1}2} & w_{j2^{m+1}3} & w_{j2^{m+1}4} & \cdots & w_{j2^{m+1}2^{m+1}-1} & w_{j2^{m+1}2^{m+1}} \end{bmatrix}_{2^{m+1} \times 2^{m+1}}$$

$$U = \begin{bmatrix} B_1 & & & \\ & B_2 & & \\ & & \cdots & \\ & & & B_{2^{(l-1)m}} \end{bmatrix}_{2^{ml+1} \times 2^{ml+1}}$$

Once the circuit is constructed as above, the computation is performed as follows.

Computation. The input at level l is a state vector of size $2^{ml+1} \times 1$ as follows: $X^T = [x_{j1}, 0, x_{j2}, 0, \dots, x_{j2^m}, 0]$, $1 \leq j \leq 2^{m(l-1)}$, where x_{jk} , $1 \leq k \leq 2^m$, are inputs to the j th gate. The operation UX computes the weighted sum of all the gates at

level l . Pass the $m+1$ least significant qubits through a $D(m+1, \delta)$ gate followed by the sink gate for m qubits (except q_0), where δ is chosen to be sufficiently small. (The exact value is specified below and depends on error bounds.) Note that this process simulates all the Et gates at one level in parallel, where U gate computes the weighted sum and the D gate acts as a zero checker.

Precision of amplitudes in the state vector x . At the lowest level of the circuit we have 2^{md} input nodes such that $\sum_{i=1}^{2^{md}} |x_i|^2 = 1$. Thus, we need a precision of at least $O(dm) = O(d \log s)$ for the state vector. Of course, after every D gate, $1/2^m$ of these states disappear. Therefore, if the amplitudes are not lost in the sink state, we need a precision of $O(l \log s)$ at level l .

Precision of weights in U gates. Let $\varepsilon_l \geq 0$ denote the error bound in weight values at level l , where the output node corresponds to level 1. As mentioned before, we need to ensure that $\varepsilon_l \leq \frac{1}{\sqrt{sw}}$ at all levels l . Let w_1, w_2, \dots, w_s be the correct normalized weights corresponding to a row of U . Let w'_1, w'_2, \dots, w'_s be the erroneous weights. Let x_j and x'_j , $1 \leq j \leq s$, respectively denote the correct and the erroneous input values corresponding to the row of U . Then,

$$\begin{aligned} \varepsilon_l &\leq \left| \sum_{j=1}^s w'_j x'_j - \sum_{j=1}^s w_j x_j \right| \\ &\leq \sum_{j=1}^s (|w_j| + \varepsilon_{l+1})(|x_j| + \varepsilon_{l+1}) - \sum_{j=1}^s |w_j| |x_j| \\ &\leq s\varepsilon_{l+1}^2 + \varepsilon_{l+1} \sum_{j=1}^s (|w_j| + |x_j|) \\ &\leq s\varepsilon_{l+1}^2 + 2\varepsilon_{l+1} \sqrt{s}, \quad \text{as } \sum_{j=1}^s |w_j|^2 = 1 \quad \text{and} \quad \sum_{j=1}^s |x_j|^2 \leq 1 \\ &\leq (\sqrt{s} \varepsilon_{l+1})^2 + 2\sqrt{s} \varepsilon_{l+1} \end{aligned}$$

If $\varepsilon_l \leq \frac{1}{3^{l/s} s^{1/2} w}$, then we have $\varepsilon_l \leq \frac{1}{\sqrt{sw}}$ for all l . Thus, the circuit needs $O(l \log s + \log w)$ precision for the weights in U gate at level l .

Threshold and precision for the D gate. The smallest integral value that can put the corresponding Et gate over the threshold is 1. The corresponding weights in QNN are normalized by dividing by $\sqrt{\sum_{k=1}^s |w_{jk}|^2} \leq \sqrt{s} w$. Also the normalized input of 1's are encoded as $\sqrt{1/2^{ml}} = 1/\sqrt{s^l}$. Therefore, we can choose $0 < \delta < 1/\sqrt{s^l} \sqrt{s} w$, a good value being $\delta = 1/2 \sqrt{s^l} \sqrt{s} w$. With error bound ε we can ensure that the amplitude values never fall in the range (δ_0, δ_1) , where $\delta_0 = \varepsilon$ and $\delta_1 = 2\delta - \varepsilon$.

The output of D gate must be within ε_l of the correct value at level l . ■

COROLLARY 4.7. $TC(n^{O(1)}, O(1)) \subseteq QNN(O(\log n), O(1))$ of precision $O(\log n)$.

Thus, $QNN(O(\log n), O(1))$ can approximate elementary functions such as sine, cosine, exponential, logarithm, and square root. It can also exactly compute integer

and polynomial quotient and remainder, interpolation of rational polynomials, banded matrix inverse, and triangular Toeplitz matrix inverse.

COROLLARY 4.8. $\text{NC}^1 \subseteq \text{QNN}(O(\log^2 n), O(\log n))$ of precision $O(\log^2 n)$.

COROLLARY 4.9. $\text{NC}^2 \subseteq \text{QNN}(O(\log^2 n), O(\log^2 n))$ of precision $O(\log^2 n)$.

Thus, $\text{QNN}(O(\log^2 n), O(\log^2 n))$ can compute various matrix operations such as inverse and rank.

COROLLARY 4.10. $\text{NC} \subseteq \text{QNN}(\log^{O(1)} n, \log^{O(1)} n)$ of precision $\log^{O(1)} n$.

COROLLARY 4.11. $\text{POLYLOGSPACE} \subseteq \text{QNN}(\log^{O(1)} n, \log^{O(1)} n)$ of precision $\log^{O(1)} n$.

Hence, the several natural problems in TC and NC can be solved using only $\log^{O(1)} n$ qubits and at most $\log^{O(1)} n$ steps.

So far the D gate was not completely defined. However, to delimit the power of QNNs, we need to define the behavior completely. For the following results, we assume that only the least significant qubit out of the D gate is not connected to the sink gate and $\mathcal{A}(|j; 1\rangle) = 0$ for all j . These assumptions ensure that the D gate is not performing difficult computations on the undefined states. The result holds if the behavior of the D gate on all the states $|i\rangle$, $1 \leq i \leq 2^m - 1$, is the same as that on the state $|0^m\rangle$.

THEOREM 4.12. $\text{QNN}(s, d)$ of precision $p \subseteq \text{EC}(\lceil d/2 \rceil 2^s, \lceil d/2 \rceil)$ of weight $O(2^{2\lceil \log s + p \rceil})$. (Read $s(n)$ and $d(n)$ for s and d , respectively.)

Proof. Replace every U gate that has k qubits as input with 2^k weighted linear adders and every D gate with a zero checker. Consecutive linear adders can be combined into one adder, and an adder followed by the zero checker can be combined into a Et gate. Thus, the depth of the EC circuit is reduced by at least half.

Since the original circuit has s qubits and depth d , we need at most 2^s equality threshold gates at each level for a total of at most $\lceil d/2 \rceil 2^s$ gates. (Multiple U gates at the same level operating on different qubits need less than 2^s gates.)

In general, the weights in the U matrix can be complex numbers while Et gates are allowed to have only integer weights. Thus, we need to ensure that both the real and imaginary parts are zero. This can be done simultaneously by scaling the imaginary part of weights by $2^{2\lceil \log s + p \rceil}$ and the real weights by $2^{\lceil \log s + p \rceil}$ and then adding them to obtain a single integer. Scaling by $2^{2\lceil \log s \rceil}$ ensures that the weighted sums of the real and imaginary parts do not mix. ■

Thus, the computational power of simplified $\text{QNN}(O(\log n), O(1))$ of precision $O(\log n)$ is the same as that of $\text{EC}(n^{O(1)}, O(1))$ of weight bound $n^{O(1)}$ and $\text{TC}(n^{O(1)}, O(1))$.

4.6. Encoders and Decoders

In the previous section, we proved that QNNs can process information in parallel if the information is presented in encoded form. However, in general, the information

may be available only in the classical form. In this case, a special apparatus needs to be built to encode n classical bits into $O(\log n)$ qubits. In this section, we show that such an apparatus is indeed feasible by demonstrating unitary matrices for encoders. These unitary matrices are highly structured, and hence, in practice their implementations may look quite different from the way it is presented here.

Encoders. Recall that we need to encode $n = 2^m$ classical bits a_i , $0 \leq i \leq n-1$, in $\log n$ qubits as $c \sum_{i=0}^{n-1} \alpha_i |i\rangle$, where $\alpha_i = a_i$, $a_i \in \{0, 1\}$, and c is an appropriate constant such as $1/\sqrt{n}$.

The unitary operator for the encoders operates on n qubits each in one of the states $|0\rangle$ or $|1\rangle$, $\log n$ qubits to be used for encoding, and an additional qubit corresponding to the environment or sink. The operator can be described as $2^{n+\log n+1} \times 2^{n+\log n+1}$ banded matrix of band size $2n \times 2n$.

$$B_{b_{n-1} \dots b_1 b_0} = c \begin{bmatrix} b_0 & e_{1,2} & \cdots & e_{1,2n} \\ 1-b_0 & e_{2,2} & \cdots & e_{2,2n} \\ b_1 & e_{3,2} & \cdots & e_{3,2n} \\ & & \cdots & \\ b_{n-1} & e_{2n-1,2} & \cdots & e_{2n-1,2n} \\ 1-b_{n-1} & e_{2n,2} & \cdots & e_{2n,2n} \end{bmatrix}_{2n \times 2n}$$

$$U_E = \begin{bmatrix} B_{00 \dots 00} & & & \\ & B_{00 \dots 01} & & \\ & & \vdots & \\ & & & B_{11 \dots 10} \\ & & & & B_{11 \dots 11} \end{bmatrix}_{2^{n+\log n+1} \times 2^{n+\log n+1}}$$

All the entries e_{jk} of $B_{b_{n-1} b_{n-2} \dots b_0}$ are chosen so that the rows form a system of orthonormal vectors. Now suppose we want to encode n classical bits a_0, a_1, \dots, a_{n-1} into $\log n$ qubits as described above. Prepare a system in the following state $|a_0, a_1, \dots, a_{n-1}; 0^{\log n}, 0\rangle$, where $0^{\log n}$ denotes the state of qubits used for encoding and the last qubit corresponds to the sink state. After the operator U_E is applied to this state, we obtain the following superposition of states: $c \sum_{i=0}^{n-1} \alpha_i |a_0, a_1, \dots, a_{n-1}; i, z\rangle$, where $\alpha_i = a_i$ if $z = 0$, and $\alpha_i = 1 - a_i$ if $z = 1$. Now send the first n qubits corresponding to the classical bits to sink gates to obtain the encoding in the $\log n$ qubits as needed.

Decoders. If the output consists of one classical bit, a simple observation of the corresponding qubit will yield the classical information. Even if there are more than 1 bit in the output, they can be observed after repeated runs of the circuit, or by having multiple copies of the circuit. Having multiple copies of the circuit has the advantage of making the computational system robust.

5. DISSIPATION GATE

In this section, we show that the behavior of the D gate can be modeled by cubic nonlinear differential equation. Similar equations are frequently used in quantum

systems of interacting particles. Though these equations are not identical to ours, we believe that they demonstrate the consistency of D gate with the laws of quantum mechanics and identify some possible approaches for implementing it. Another significant aspect of the D gate is irreversibility. To achieve this *dissipative* property in a quantum system, it is necessary to introduce some kind of controlled interaction with, say, an environment [11]. Designing specific mechanisms, though possible in principle, will not be facile.

5.1. Amplitude Evolution Equation

We show that the dynamical behavior of the D gate on the amplitude of state $|0^m\rangle$ can be achieved by cubic nonlinearities using stable points 0 and 1. Since it is irrelevant what happens to states other than $|0^m\rangle$, for simplicity, let us denote $\mathcal{A}(|0^m\rangle)$ by \mathcal{A} . (Indeed, the amplitudes of all the states can evolve as follows without affecting our results.) The differential equation that describes the required behavior is

$$\frac{d}{dt} \mathcal{A} = R\mathcal{A}(|\mathcal{A}| - \delta)(1 - |\mathcal{A}|), \quad (1)$$

where R denotes the rate of convergence. It is clear that the phase of \mathcal{A} remains invariant under this evolution and only its amplitude is a dynamical variable. So, let us focus on $a \equiv |\mathcal{A}|$. Note that $\frac{da}{dt}$ is negative in the range $(0, \delta)$ and positive in the range $(\delta, 1)$. Thus, a monotonically decreases in the range $(0, \delta)$ and monotonically increases in the range $(\delta, 1)$. Also, the derivative $\frac{da}{dt}$ is 0 at points 0, δ , 1, and therefore, a does not change at these points.

Let a_0 denote the initial value of a . Then the explicit solution to Eq. (1) is

$$\left(\frac{a}{a_0}\right)^{1/\delta} \left(\frac{a-\delta}{a_0-\delta}\right)^{-1/\delta(1-\delta)} \left(\frac{1-a}{1-a_0}\right)^{1/(1-\delta)} = e^{-Rt}. \quad (2)$$

Alternative forms, convenient for analyzing the behavior near the points 0, δ , 1, may be obtained by raising both sides to the appropriate power. For example, near 0, we may write

$$\left(\frac{a}{a_0}\right) \left(\frac{a-\delta}{a_0-\delta}\right)^{-1/(1-\delta)} \left(\frac{1-a}{1-a_0}\right)^{\delta/(1-\delta)} = e^{-\delta Rt} \quad (3)$$

for convenience.

If $a_0 \neq \delta$ and $t \rightarrow \infty$, the right side of the equation tends to 0. Since a monotonically decreases in the range $(0, \delta)$ and monotonically increases in the range $(\delta, 1)$, it converges to 0 or 1 as $t \rightarrow \infty$, depending on whether it started below or above δ respectively.

5.2. Convergence Time

Suppose the system is set up so that amplitudes never fall in the range (δ_0, δ_1) , where $0 \leq \delta_0 < \delta < \delta_1 \leq 1$. The specific values δ_0 and δ_1 depend on the properties of quantum neural network (QNN) which, in turn, depends on the problems we are trying to solve.

The next question is what should be the rate of convergence, R , so that the fixed points 0 and 1 are reached with tolerance ε within some finite time T . Demanding both

$$a(T) < \varepsilon \quad \text{if } a(0) < \delta_0 \quad (4)$$

$$1 - a(T) < \varepsilon \quad \text{if } a(0) > \delta_1, \quad (5)$$

we obtain two equations by substituting $a = \varepsilon$, $s = \delta_0$ and $a = 1 - \varepsilon$, $s = \delta_1$ in Eq. (2). The two equations provide two rates R_0 and R_1 , for $a < \delta_0$ and $a > \delta_1$, respectively. For our purposes, it is sufficient to choose $R = \max(R_0, R_1)$ so that both inequalities (4, 5) are satisfied. Thus, given δ_0 , δ_1 , δ , ε and time T , we obtain the parameters of the system needed to implement the D gate.

The evolution described so far converges $|\mathcal{A}(|0^m\rangle)|$ to 0 or 1 without changing the phase of the state. In the next step we collapse $\mathcal{A}(|0^m\rangle)$ to 0 or 1.

5.3. Dissipation

Once the amplitude $|\mathcal{A}(|0^m\rangle)|$ converges close to 0 or 1, the quantum system is measured along state $|0^m\rangle$. The measurement collapses the system to state $|0^m\rangle$ with a high probability if $|\mathcal{A}(|0^m\rangle)|^2$ is close to 1. Note that this part of the D operator is also dissipative and irreversible. We envisage interactions of our quantum system with an environment, in a controlled fashion, can produce both the nonlinearities and the collapse needed to construct the D gate.

What happens if the system is observed along state $|0^m\rangle$ and $|\mathcal{A}(|0^m\rangle)|^2 = 0$? This situation occurs when say a photon in state $|\rightarrow\rangle$ is observed using an orthogonal filter $|\uparrow\rangle$ —nothing is observed. This difficulty is easily addressed while solving another problem described below.

In general, the m qubits passed through the D gate are part of a larger computing system of $m \leq n$ qubits. In this case, we demand the above nonlinear behavior of the D gate on all $|j; 0^m\rangle$ states, for $0 \leq j \leq 2^{n-m} - 1$. This general behavior presents the following difficulty. It is possible that $\sum_{j=0}^{2^{n-m}-1} |\mathcal{A}(|j; 0^m\rangle)|^2 < \sum_{j=0}^{2^{n-m}-1} \sum_{k=1}^{2^m} |\mathcal{A}(|j; k\rangle)|^2$, and hence, when the system is measured along state $|0^m\rangle$, it does not collapse to state $|0^m\rangle$ as needed.

To solve the above problem, we introduce an ancilla qubit z in state $|0\rangle$ so that $\mathcal{A}(|j; k; 1\rangle) = 0$ for $0 \leq j \leq 2^{n-m} - 1$ and $0 \leq k \leq 2^m - 1$. Once the amplitudes $\mathcal{A}(|j; 0^m; 0\rangle)$ have converged close to 0 or 1, transfer the amplitude of state $|j; 0^{m-1}; 0\rangle$ to state $|j; 0^m; 1\rangle$ for all $0 \leq j \leq 2^{n-m} - 1$. This operation on the last of the m qubits and the qubit z is performed using the following 4×4 unitary operator.

$$U = \begin{bmatrix} 1 & 0 & 0 & 0 \\ 0 & 0 & 1 & 0 \\ 0 & 1 & 0 & 0 \\ 0 & 0 & 0 & 1 \end{bmatrix} \begin{matrix} |00\rangle \\ |01\rangle \\ |10\rangle \\ |11\rangle \end{matrix}.$$

The operator U changes the state for the last qubit and the ancilla qubit from $[b_0, 0, b_2, 0]$ to $[b_0, b_2, 0, 0]$ so that when the last qubit is measured along $|0\rangle$, it collapses to state $|0\rangle$ as $\mathcal{A}(|j; 0^{m-1}1; z\rangle) = 0$ for all $0 \leq j \leq 2^{n-m}-1$ and $0 \leq z \leq 1$. Of course, the above unitary behavior and interaction with an environment can be built in the D gate without requiring a separate operator.

If we need to collapse all the m qubits to the state $|0^m\rangle$, the above process can be executed for all the m qubits. However, to solve the many problems described in this paper, we do not need to do so. All except the last of the m qubits are discarded to solve these problems. Thus, it is irrelevant what happens to the other $m-1$ qubits when we observe them.

Next we describe some simple quantum systems that can be modeled using cubic nonlinearities. While the equations for these systems are different from Eq. (1), they demonstrate that cubic nonlinearities are common in modeling quantum systems and indicate some possible approaches for implementing the D gate. Furthermore, these models clearly demonstrate that we have not tapped the full power of quantum systems available to us.

6. NONLINEARITIES IN QUANTUM MECHANICAL SYSTEMS

In this section, we address the question of nonlinearities in quantum mechanics. While it is generally believed that, at the fundamental level, the evolution of the entire universe is governed by a linear Schrödinger's equation for "the wavefunction of the universe," this view is not particularly helpful in practice. For limited physical systems, such as those found in our laboratories, the linear Schrödinger's equation is only an approximation where certain degrees of freedom can be ignored or controlled. Thus, in the most celebrated example, an electron in a hydrogen atom, we find [36]

$$i\hbar \frac{\partial \psi(\mathbf{x}, t)}{\partial t} = \left[-\frac{\hbar^2}{2m} \nabla^2 - \frac{e^2}{r} \right] \psi(\mathbf{x}, t), \quad (6)$$

where $2\pi\hbar$ is the Planck's constant, $\psi(\mathbf{x}, t)$ is the wave function (probability amplitude) associated with the electron at space-time point (\mathbf{x}, t) , m is the electron mass, e the elementary charge, and r is the magnitude $|\mathbf{x}|$. Here, the nucleus (proton) has been placed at the origin of the coordinate system, providing only an "external," Coulomb potential (e^2/r) in which the electron moves. All the degrees of freedom associated with the proton are ignored in this equation. In fact, it is treated as a *classical* particle. Had we taken into account its quantum mechanical properties, or the fact that it is composed of three quarks, we would have to consider wave functions for these and to deal with the associated equations. The resultant would be far more complex than Eq. (6). Similarly, the Coulomb potential is known to be one

aspect of a photon, so that its degree of freedom has also been *ignored* in this simple equation. If the quantum mechanics of the photon is also taken into account, we are necessarily faced with the full theory of relativistic quantum fields [21]. The most venerable example of such kind of system is quantum electrodynamics [16, 21], in which *interactions* between the electrons and photons are fully incorporated. Nevertheless, by ignoring all degrees of freedom except that associated with the electronic position, a simple linear equation such as (6) has been used to predict many properties of the hydrogen atom, to a high degree of accuracy. Parenthetically, notice that the spin degree of freedom, a favorite in quantum computing community, is also ignored in Eq. (6). When this is included into a more complex version of Eq. (6), the effects of “spin-orbit” coupling can be discussed and a better approximation of the properties of hydrogen emerges.

Between the simplest levels of approximation, such as Eq. (6), and the most complete/complex theories lies a vast set of approaches. Instead of simply ignoring some of the other degrees of freedom, these “intermediate” theories incorporate some of their effects into “effective interactions.” The results involve, typically, nonlinear equations. We give two examples here.

An early example, predating quantum electrodynamics, takes into account the “self interaction” of the electron in, say, the hydrogen atom. The idea is that, since quantum mechanical description of the electron is in terms of a probability distribution, $P(\mathbf{x}) = |\psi(\mathbf{x})|^2$ (where we have dropped the t dependence for simplicity), we are faced with a charge distribution associated with this electron: $\rho(\mathbf{x}) = -eP(\mathbf{x})$, i.e.,

$$\rho(\mathbf{x}) = -e |\psi(\mathbf{x})|^2. \quad (7)$$

By the known laws of electrodynamics [20], this charged cloud would generate an electric potential, at every point in space, \mathbf{x} , of the form

$$V_\rho(\mathbf{x}) = \int \frac{\rho(\mathbf{x}')}{|\mathbf{x} - \mathbf{x}'|} d\mathbf{x}'. \quad (8)$$

But then this potential should affect the electron in a way no different than the potential due to the proton (that is, the e^2/r term in Eq. (6)). Inserting this extra potential into (6), we have

$$i\hbar \frac{\partial \psi(\mathbf{x}, t)}{\partial t} = \left[-\frac{\hbar^2}{2m} \nabla^2 - \frac{e^2}{r} - eV_\rho(\mathbf{x}) \right] \psi(\mathbf{x}, t). \quad (9)$$

Combining Eqs. (7), (8) and (9), we arrive at a Schrödinger’s equation with cubic nonlinearity:

$$i\hbar \frac{\partial \psi(\mathbf{x}, t)}{\partial t} = \left[-\frac{\hbar^2}{2m} \nabla^2 - \frac{e^2}{r} \right] \psi(\mathbf{x}, t) + e^2 \int \frac{\psi(\mathbf{x}, t) |\psi(\mathbf{x}', t)|^2}{|\mathbf{x} - \mathbf{x}'|} d\mathbf{x}'. \quad (10)$$

Notice that the last term describes the electron’s interaction with *itself*, as the source of the potential is the electronic cloud. We should emphasize that this equation was

eventually abandoned for a number of reasons. One of them is that, as an approximation which keeps only the electronic degree of freedom (ψ) while ignoring the photonic degree of freedom, it is too crude to describe self interaction adequately. As mentioned above, quantum electrodynamics was developed and the final picture is not simply embodied in Eq. (10).

Another example, which is similar in form, comes from the study of structure of atoms with more than one electron. Instead of self interactions, the interest here is the *mutual* interactions between the electrons. Known as the Hartree approximation, with the photonic degrees of freedom still ignored, a system of nonlinear Schrödinger equations are used, even today (see Schiff [35], Section 47):

$$i\hbar \frac{\partial}{\partial t} \psi_k(\mathbf{x}_k, t) = \left[-\frac{\hbar}{2m} \nabla_k^2 - \frac{Ze^2}{|\mathbf{x}_k|} + \sum_{j \neq k} \int |\psi_j(\mathbf{x}_j)|^2 \frac{e^2}{r_{jk}} d\mathbf{x}_j \right] \psi_k(\mathbf{x}_k, t). \quad (11)$$

Here, $\psi_k(\mathbf{x}_k, t)$ is the wave function of the k th electron in an atom with Z electrons (and Z protons in the nucleus) and $r_{jk} = |\mathbf{x}_j - \mathbf{x}_k|$ is the distance between it and the j th electron. Notice that this is a system of Z nonlinear integrodifferential equations for the Z unknowns $\psi_k(\mathbf{x}_k, t)$.

Both of these examples illustrate the use of nonlinear Schrödinger equations (up to cubic terms) in the context of quantum mechanical systems. Very similar equations are also used in the context of nonlinear optics. In fact, many of these are even closer in form to the ones we proposed, for example,

$$\frac{\partial}{\partial t} \mathcal{A}(t) = c_1 \mathcal{A} + c_3 |\mathcal{A}|^2 \mathcal{A}, \quad (12)$$

where c_1 and c_3 are constants ([10], p. 280). Similarly, nonlinear Schrödinger equations of this type appear frequently in the study of solitons [19]. Finally, known as the time-dependent Landau–Ginzburg equation, nonlinear systems of the form of (12) are ubiquitous in many areas of condensed matter physics.

In elementary quantum mechanics, the equations of evolution tend to be linear in the wave function, describing various degrees of freedom (such as spins) subjected to *external* potentials. However, as soon as *internal* interactions between the degrees of freedom we wish to describe are incorporated, nonlinearities are inevitable. This section serves to illustrate that evolution of many physical systems are governed by nonlinear equations. Since the equations governing the D gate are sufficiently similar to many of those in physical systems, we believe that its implementation should be possible.

7. RESEARCH DIRECTIONS

This paper initiates research into what problems can be solved using only polylogarithmic ($\log^{O(1)} n$) entangled qubits and at most polylogarithmic steps. All the efforts so far have concentrated on what can be achieved using a polynomial number of qubits. We have shown that constant depth QNNs of logarithmic size have the same computational power as threshold circuits of polynomial size and

constant depth, which are used for modeling neural networks. QNNs possess several advantages over threshold circuits. First, we need only $O(\log n)$ qubits. Second, there is no communication bottleneck and synchronization problems associated with computing the weighted sum in a threshold gate; there is no need to explicitly wire the entangled qubits together and the synchronization is instantaneous for the computation of the weighted sum. Finally, quantum systems have the ability to compute on probability distributions rather than just discrete values, giving them the ability to handle fuzzy sets [43].

The research suggests several interesting directions.

1. Define a continuous version of QNNs using probability amplitude distributions. Quantum mechanics uses infinite-dimensional Hilbert spaces to model reality. (Even a simple system such as an electron around a nucleus in a hydrogen atom is modeled using infinite-dimensional Hilbert space.) How can this be used to generalize the discrete model discussed in this paper? What kind of gates/operators are allowed? Just as we used discrete values to encode boolean values, we can use the continuous distribution to encode membership in fuzzy sets [43].

2. How can error-correcting codes and fault-tolerant computing be adapted to the new model, both for the discrete and continuous versions?

3. Following the road map provided by the theory of neural networks, define a theory of $\text{QNN}(\log^{O(1)} n, \log^{O(1)} n)$. What is the equivalent of back-propagation and various other supervised and unsupervised learning algorithms? What is the equivalent of the Hopfield model and recurrent neural networks? How can we define the formal statistical mechanics of QNNs?

4. Matrix operations provide the “killer application” for the new model. Improve the bounds on our results: $\text{TC}^0 \subseteq \text{QNN}(O(\log n), O(1))$ and $\text{NC} \subseteq \text{QNN}(\log^{O(1)} n, \log^{O(1)} n)$. In particular, minimizing the depth of the circuits can provide real-time solutions to several important matrix problems. Reducing the depth of the circuits to a constant, even at the expense of increasing the size, can provide real-time solutions to problems in POLYLOGSPACE . The results in this paper do not take advantage of either complex probability amplitudes as weights, or arbitrary unitary operators. (This paper uses banded unitary matrices with real weights to perform simulations.) Also, can we get better bounds under various uniformity constraints?

Of course, with polylogarithmic size and precision, the quantum system has more than a polynomial number of states, and hence, it may be infeasible to set up the required apparatus in reasonable time. Thus, such computational systems may be more appropriate in the context of learning systems, where the parameters are incrementally modified based on how the actual output of the system differs from the required output.

5. Understand the physics behind the implementation of the new operators. What other operators are allowed for the discrete as well as the continuous model of QNNs? How can they be physically realized? For example, we can define “generalized D gates” that behave on all the states $|i\rangle$, $1 \leq i \leq 2^m - 1$, as the D gate behaves on the state $|0^m\rangle$ using similar evolutionary equation.

6. Develop a theory of EC circuits. While threshold circuits have been studied extensively and the computational power of EC circuits is essentially same as the power of threshold circuits (with polynomial size), it is not at all clear that the *learning strategies* are essentially the same. First, EC circuits can be naturally defined over the domain of complex numbers. We need to explore how this larger domain helps. Second when translated to QNNs, EC circuits must have normalized weights, which means that the learning algorithms such as back-propagation that make local changes to weights, cannot be directly translated without some form of global strategy. Third, for every gate in an EC circuit, QNNs have weight vectors orthogonal to the original one. In this paper, these vectors simply dissipate after the D operator and sink gates. However, they may indeed be helpful in obtaining better learning algorithms. Thus, investigating EC circuits with normalized complex weights and orthogonal weight vectors is important, independent of their connection to quantum computing.

7. Compare QNNs with the existing data in neuroscience to improve our understanding of biological neurons and, if necessary, to refine our model. It is well-known that all creatures with nervous systems have essentially the same basic processing unit, the biological neuron, though different types of neurons have been identified possessing the same general structure. The dendrites on the cell body receive inputs from several neurons, the signal is processed in the cell body and a long axon, and is output on the other side. Reaction time of the lower brain for many nontrivial tasks is less than 100s, while the synapse response time of most neurons is at least 5s. Thus, biological evidence suggests that the depth of these circuits cannot exceed 20.

It is well known that the synaptic connections change as the brain learns. However, there is almost no experimental evidence of a neuron changing from an excitatory to inhibitory or vice versa as the learning occurs. In fact, this is one of the factors cited against artificial neural networks (threshold circuits) and the associated learning algorithms where the weights associated with synaptic connections can change from positive to negative.

Thus, it is possible that the unitary operator U is associated with the synapses while the dissipation operator D is associated with the cell and the axon. Hence, the synapses are not computing on classical bits associated with the input but the quantum interactions between the neurotransmitters received at the input. Note that the reality is more complicated than this simplistic model. It has been observed that the neurons fire a series of spikes and information may be encoded in the rate and timing of firing as well [24]. Of course, if we allow feedback in QNNs, the timing issues must be considered. The possibility of the information being encoded in the interactions of these carriers needs to be investigated.

ACKNOWLEDGMENT

The author is indebted to Harald Hempel for carefully reading the first draft of the paper and suggesting numerous improvements.

REFERENCES

1. D. S. Abrams and S. Lloyd, Nonlinear quantum mechanics implies polynomial-time solution for NP-complete and #P problems, *Phys. Rev. Lett.* **81** (1998), 3992–3995.
2. D. Aharonov, Quantum computation, 1998. [<http://xxx.lanl.gov/ps/quant-ph/9812037>]
3. E. Allender and U. Hertrampf, Depth reductions for circuits of unbounded fan-in. *SIAM J. Comput.* **112** (1994), 217–238. [An earlier version appears as: E. Allender, A note on the power of threshold circuits, *Found. Comput. Sci.* (1989), 580–584]
4. A. Bavenço, C. Bennet, R. Cleve, D. DiVincenzo, N. Margolus, P. W. Shor, T. Sleator, J. Smolin, and H. Weinfurter, Elementary gates for quantum computation, *Phys. Rev. A* **52** (1995), 34–57.
5. P. A. Benioff, Quantum mechanical Hamiltonian models of Turing machines, *J. Statist. Phys.* **29**(3) (1982), 515–546.
6. C. H. Bennett, Logical reversibility of computation, *IBM J. Res. Development* **17** (1973), 525–532.
7. C. H. Bennett, Time/space trade-offs for reversible computation, *SIAM J. Comput.* **18** (1989), 766–776.
8. E. Bernstein and U. Vazirani, Quantum complexity theory, *SIAM J. Comput.* **26**(5) (1997), 1411–1473.
9. A. Berthiaume, Quantum computation, in “Complexity Theory Retrospective II” (L. A. Hemaspaandra and A. L. Selman, Eds.) Chap. 2, pp. 23–51, Springer-Verlag, Berlin, 1997.
10. R. W. Boyd, “Nonlinear Optics,” Academic Press, San Diego, 1991.
11. A. O. Caldeira and A. J. Leggett, Quantum tunneling in a dissipative system, *Ann. Phys.* **149** (1983), 347–456.
12. R. Cleve and J. Watrous, Fast parallel circuits for the quantum fourier transform, 2000. [<http://xxx.lanl.gov/ps/quant-ph/0006004>]
13. D. Deutsch, Quantum theory, the Church–Turing principle and the universal quantum computer, *Proc. R. Soc. London A* **400** (1985), 97–117.
14. D. Deutsch, Quantum computational networks, *Proc. R. Soc. London A* **425** (1989), 73–90.
15. R. P. Feynman, Simulating physics with computers, *Int. J. Theor. Phys.* **21**(6/7) (1982), 467–488.
16. R. P. Feynman, “Quantum Electrodynamics,” Perseus Press, New York, 1998.
17. F. Green, S. Homer, and C. Pollett, On the complexity of quantum ACC., 2000. [<http://xxx.lanl.gov/ps/quant-ph/0002057>]
18. J. Gruska, “Quantum Computing,” McGraw–Hill, London, 1999.
19. E. Atlee Jackson, “Perspectives of Nonlinear Dynamics,” Cambridge, Univ. Press, Cambridge, UK, 1991.
20. J. D. Jackson, “Classical Electrodynamics,” Wiley, New York, 1998.
21. M. Kaku, “Quantum Field theory: A Modern Introduction,” Oxford Univ. Press, London, 1993.
22. D. Kozen, “The Design and Analysis of Algorithms,” Texts and Monographs in Computer Science, Springer-Verlag, Berlin/New York, 1991.
23. R. Landauer, Is quantum mechanics useful? *Phil. Trans. R. Soc. Lond. A* **353** (1995), 367–376.
24. W. Maass and C. M. Bishop, “Pulsed Neural Networks,” MIT Press, Cambridge, MA, 1999.
25. W. S. McCulloch and W. Pitts, A Logical calculus of the ideas immanent in nervous activity, *Bull. Math. Biophys.* **5** (1943), 115–133.
26. W. S. McCulloch and W. Pitts, How we know universals, *Bull. Math. Biophys.* (1947), 127–147.
27. C. Moore, Quantum circuits: Fanout, parity and counting, 1999. [<http://xxx.lanl.gov/ps/quant-ph/9903046>]
28. C. Moore and M. Nilsson, Parallel quantum computation and quantum codes, 1998. [<http://xxx.lanl.gov/ps/quant-ph/9808027>]
29. J. Preskill, Physics 229. [<http://www.theory.caltech.edu/people/preskill/ph229>]

30. J. Preskill, Fault-tolerant quantum computation, 1997. [<http://xxx.lanl.gov/ps/quant-ph/9712048>]
31. J. H. Reif, "Synthesis of Parallel Algorithms," Morgan Kaufmann, San Mateo, CA, 1993.
32. J. H. Reif and S. R. Tate, On threshold circuits and polynomial computation, *SIAM J. Comput.* **21**(5) (1992), 896–908.
33. E. G. Reiffel and W. Polak, An introduction to quantum computing for non-physicists, 1998. [<http://xxx.lanl.gov/ps/quant-ph/9809016>]
34. A. Borodin, On relating time and space to size and depth, *SIAM J. Comput.* **6**(4) (1977), 733–744.
35. L. I. Schiff, "Quantum Mechanics," McGraw-Hill, New York, 1968.
36. R. Shankar, "Principles of Quantum Mechanics," Plenum, New York, 1994.
37. P. W. Shor, Polynomial-time algorithms for prime factorization and discrete logarithms on a quantum computer, *SIAM J. Comput.* **26**(5) (1997), 1484–1509.
38. A. Steane, Quantum computing, *Rept. Prog. Phys.* **61** (1998), 117–173.
39. W. G. Unruh, Maintaining coherence in quantum computers, *Phys. Rev. A* **51** (1995), 992–997.
40. U. Vazirani, Quantum computing. [<http://www.cs.berkeley.edu/~vazirani/qc.html>]
41. C. P. Williams and S. H. Clearwater, "Explorations in Quantum Computing," Springer-Verlag, Berlin/New York, 1998.
42. A. Yao, Quantum circuit complexity, in "Proceedings of the 34th IEEE Symposium on Foundations of Computer Science," pp. 352–361, 1993.
43. L. A. Zadeh, Fuzzy sets, *Inform. and Control* **8** (1965), 338–353.